GA–A22901

HIGH MODE NUMBER MHD STABILITY AT THE EDGE OF A TOKAMAK

by
R.L. MILLER, J.W. CONNOR, J.R. FERRON, R.J. HASTIE, L.L. LAO, T.S. OSBORNE, T.S. TAYLOR, and H.R. WILSON

JULY 1998

DISCLAIMER

GA–A22901

HIGH MODE NUMBER MHD STABILITY AT THE EDGE OF A TOKAMAK

by
R.L. MILLER, J.W. CONNOR,† J.R. FERRON, R.J. HASTIE,† L.L. LAO,
T.S. OSBORNE, T.S. TAYLOR, and H.R. WILSON†

This is a preprint of a paper to be presented at the 25th European Physical Society Conference on Controlled Fusion and Plasma Physics, June 29–July 3, 1998, Prague, Czech Republic, and to be published in the *Proceedings.*

†UKAEA Fusion Culham Science Center

Work supported by
the U.S. Department of Energy
under Grant DE-FG03-95ER54309 and the UK Department
of Trade and Industry and Euratom

GA PROJECT 3726
JULY 1998

HIGH MODE NUMBER MHD STABILITY AT THE EDGE OF A TOKAMAK*

R.L. Miller, J.W. Connor,† J.R. Ferron, R.J. Hastie,† L.L. Lao, T.S. Osborne, T.S. Taylor, and H.R. Wilson†

General Atomics, P.O. Box 85608, San Diego, CA 92186-5608

Tokamak performance is often controlled by stability of the edge plasma. Consistent with "stiff" transport models, the confinement in tokamak discharges is strongly correlated with the magnitude of the edge pressure pedestal which is limited by MHD stability. Edge stability determines the maximum sustainable pressure gradient at the edge and is believed to be responsible, at least in part, for ELM behavior. High mode number ballooning stability appears to be insufficient to explain edge observations. The local pressure gradient near the boundary in DIII–D ELMing H–mode discharges may exceed the first regime ideal ballooning limit by as much as a factor of two [1]. This disagreement between theory and experiment may be resolved by the inclusion of the self-consistent bootstrap current in the analysis [2]. However, the inclusion of edge current density is destabilizing for peeling modes [3].

Recently researchers at Culham [4,5,6] developed a high-mode-number peeling/ballooning mode model at the tokamak edge in which a critical role is played by the edge current density. The bootstrap current density, with its dependence upon pressure gradient and collisionality, is then an important element of any realistic edge stability calculation. When ohmic and bootstrap current effects are included, this model suggests a power threshold for L–H transitions and provides a plausible explanation for an ELM cycle. This edge model was originally cast in a large aspect ratio circular geometry [6]. Here we extend the analysis to finite aspect ratio and non-circular geometry. The effects of plasma shape are studied using local equilibrium models [7,8] and reconstructed experimental equilibria for direct comparison with experiment. This edge model describes the interaction of peeling mode (current driven) and ballooning mode (pressure driven) effects at high, but finite, mode number. The peeling mode criterion [6,3] for stability is given by

$$\sqrt{1-4D_M} > 1 + \frac{2}{2\pi q'} \oint \frac{J_{\|}B}{R^2 B_p^3} dl_p \tag{1}$$

where D_M is the Mercier quantity, and $D_M < 1/4$ is required for stability to interchange modes. The destabilizing effect of positive parallel current density is evident. This criterion was developed assuming a mode structure highly localized at the edge of the plasma, an assumption which the full code tests. At large pressure gradients, the ballooning mode becomes important, but the conventional ballooning mode formalism is invalid at the plasma edge. The edge model correctly accounts for the plasma edge and determines that $\sim n^{1/3}$ poloidal harmonics couple [4,5,6] to form a mode as compared with $\sim n^{1/2}$ poloidal harmonics for the conventional mode.

---

*Work supported by U.S. Department of Energy under Grant No. DE-FG03-95ER54309 and the UK Department of Trade and Industry and Euratom.

†UKAEA Fusion Culham Science Center (UKAEA/Euratom Fusion Association), Abingdon, Oxfordshire, OX14 3DB, UK

A 2D eigenvalue code has been written to determine the marginal edge current density or the marginal magnetic shear s for high mode numbers, based upon high n expansion of δW of Connor, Hastie, and Taylor [9]. Here, because the modes reach the edge of the plasma, a surface contribution arises from an integration by parts, and a vacuum contribution is present as well. A set of 1D Euler Lagrange equations for the Fourier amplitudes of the radial displacement is obtained. The boundary conditions on these differential equations are obtained from a minimization of δW. The vacuum matrix is computed from a modified version of a code by A. Pletzer [10]. The code is constructed in such a way that additional physics effects such as rotation may be added and further terms can be included to accurately treat intermediate mode numbers.

Since the modes we wish to analyze are localized to the edge region, only localized equilibrium information is required. We use a localized equilibrium model [8] for circular or dee-shaped plasmas which requires a total of nine parameters including aspect ratio, height to width, triangularity, magnetic shear s, and normalized pressure gradient α. The code can also treat full 2D numerically generated equilibria.

In Fig. 1 we show a number of results for two circular equilibria at aspect ratio A=1000 and A=3 in s-α space. The infinite-n ballooning s-α curve is shown for each. The nose of the s-α diagram for the A=3 case is at significantly higher s, due to the larger magnetic well at low aspect ratio, $D_M \sim \frac{\alpha}{s^2}\varepsilon(1-\frac{1}{q^2})$ where ε is the inverse aspect ratio. Also shown for each case is the peeling mode criterion, Eq. (1). The larger negative slope of the criterion for the A=3 equilibrium is due to the larger magnetic well. The solid curves are the edge code results with toroidal mode number, n=20. At low α the modes follow the peeling mode boundary and at large α approximate the infinite-n ballooning mode boundary. As anticipated, these results are similar to the previously studied s-α model [6].

In Fig. 2(a,b) are two unstable eigenmodes for the A=3 case for low and high values of α respectively. At low α, the peeling mode character is evident, while at large α, significant mode coupling arises for the ballooning mode.

A number of models have been put forward to explain ELM behavior. A recent survey was given by Connor [11]. The stability diagram in Fig. 1 suggests one such model for Type I Elms [6]. This is shown schematically in Fig. 3 in J_{edge}-α space where J_{edge} is the edge

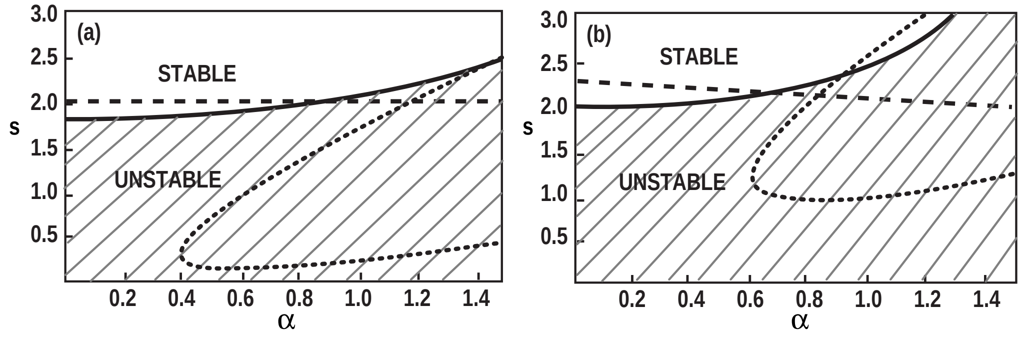

Fig. 1 Separate peeling stability boundary, infinite n ballooning stability boundary, and combined stability boundary for n=20 using the edge code for a) A=1000 and b) A=3. The shading indicates the unstable region determined by the edge code. Inside the dotted curve is unstable to infinite n ballooning; beneath the dashed line is unstable to the peeling mode.

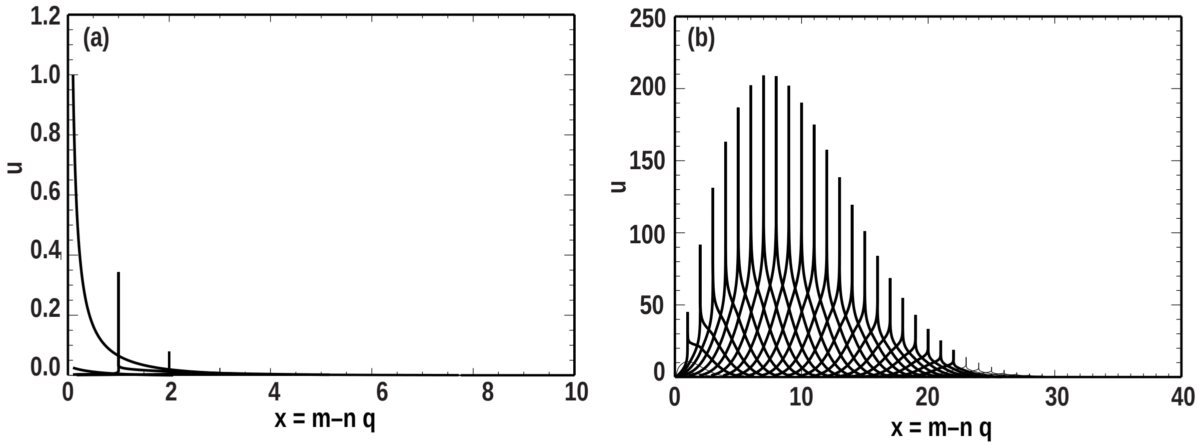

Fig.2 Unstable eigenmodes for A=3 at a) α=0.1 and b) α=1.1

current density. In general, a flux-surface averaged $J_{edge} \propto \ < J \cdot B|\nabla\psi|^{-2} >$ is linearly related to the shear, $J_{edge}=C_1-C_2$ s. For the s-α model circular equilibrium $J_{edge}/J_{ave}=1-s/2$. In phase 1, heating at the edge raises the pressure gradient and a transition to marginally stable large pressure gradient occurs. In phase 2, on a slower resistive time scale, bootstrap and ohmic currents rise and marginal stability is maintained by a slight reduction of pressure gradient. In phase 3, a continued increase of edge current cannot be stabilized at large pressure gradient, the plasma evolves into the unstable region and a Type I ELM crash occurs.

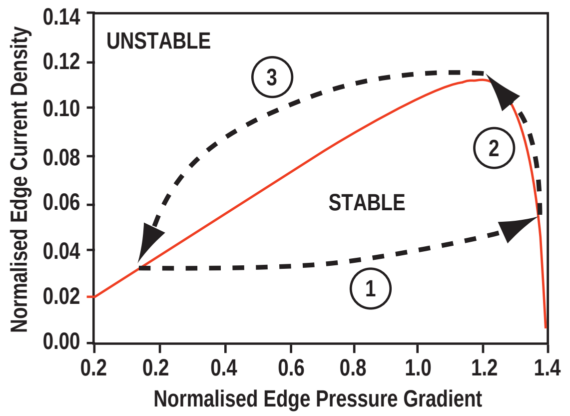

Fig. 3 Model for Type I ELM. Evolution along paths 1 and 2 are stable. Onset of instability at beginning of phase 3.

One characteristic of the stability diagram for peeling/ballooning modes as shown in Fig. 1 is that there appears to be no access to second stability. This is due to the rather weak magnetic well, even at A=3, which makes the peeling mode relatively insensitive to α and places the nose of the s-α ballooning diagram at a somewhat low value of s. However, more strongly shaped equilibria do exhibit second stable access. Stability results for A=3, κ=1.8, δ=0.5 are shown in Fig. 4(a). In this case the peeling mode stability boundary is seen to pass under the nose of the infinite-n s-α ballooning boundary. Calculation with the full edge code shows access to large α as well. In Fig. 4(b) the marginally stable eigenmode at α=3 shows that the mode is still essentially peeling although there is significant mode coupling.

We have calculated the separate ballooning and peeling stability of several DIII–D experimental equilibria. With the inclusion of the peeling mode, not all of these equilibria possess access to the second stability regime and the experimental shear values lie near the boundary of the peeling mode. The calculated loss of second regime access in highly squared plasmas, for example, may help to explain the experimentally observed higher frequency ELMs and reduced edge pressure gradient of these discharges.

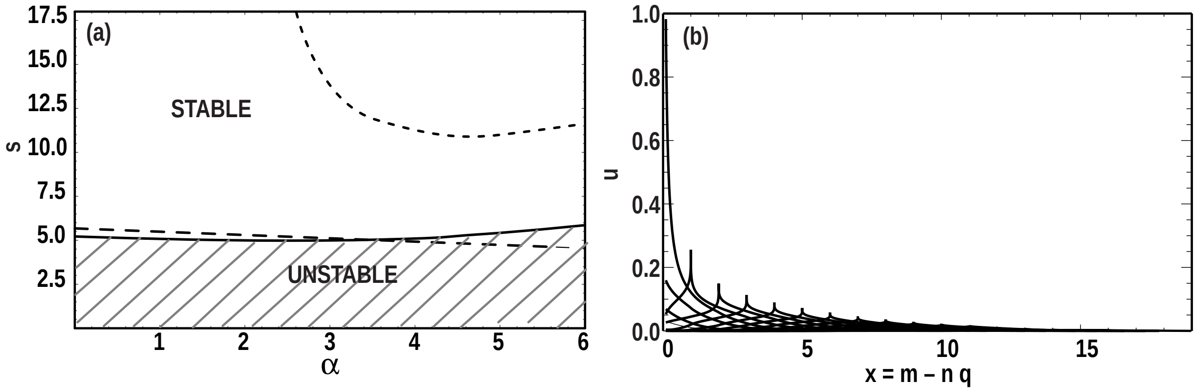

Fig.4 A=3 dee with κ=1.8 δ=0.5 stability a) s-α diagram, b) eigenmode at s=4.98 α=3. Code results used 28 poloidal harmonics which may be insufficient above α~4.

In summary, A 2D δW edge code has been constructed that analyzes edge modes not addressed by the traditional low-n δW codes nor the high-n ballooning codes. Ideal MHD stability calculated for high n localized near the edge of the plasma show peeling behavior at low α, driven by toroidal current, with a transition to modified ballooning behavior at high α. With sufficient magnetic well, second stable access is possible. Stability diagrams suggest a possible model for Type I ELMS.

The inclusion of a separatrix, a future development planned in this work, will introduce two new effects: every resonant surface occurs inside the plasma boundary and even at high toroidal mode number, n, the variation of q and s across the mode width will be large.

References

[1] T.H. Osborne *et al.*, “Scaling of ELM and H–mode pedestal characteristics in ITER shape discharges in the DIII–D tokamak,” Proc. of the Twenty Fourth European Physical Society Conference on Controlled Fusion and Plasma Physics, Berchtesgaden (European Physical Society, 1997) Part III, 289.

[2] R.L. Miller, Y.R. Lin-Liu, T.H. Osborne, T.S. Taylor, Plasma Phys. Control. Fusion **40** 753 (1998).

[3] D. Lortz, Nucl. Fusion **15** (1975) 49.

[4] J.W. Connor and H.R. Wilson,'Theory of Fusion Plasmas', Varenna (eds. J.W. Connor, E. Sindoni and J. Vaclavik) (Editrice Compositori, Bologna, 1997) 441.

[5] H.R. Wilson and J.W. Connor, Proc. of the Twenty Fourth European Physical Society Conference on Controlled Fusion and Plasma Physics, Berchtesgaden (European Physical Society, 1997) Part I, 289.

[6] J.W. Connor, R.J. Hastie, and H.R. Wilson, UKAEA FUS 383 November 1997; J.W. Connor, R.J. Hastie, H.R. Wilson, and R.L. Miller, to be published in Physics of Plasmas.

[7] C.M. Bishop, P. Kirby, J.W. Connor, R.J. Hastie, and J.B. Taylor, Nucl. Fusion **24** 1579 (1984).

[8] R.L. Miller, M.S. Chu, J.M. Greene, Y.R. Lin-Liu, and R.E. Waltz, Phys. Plasmas **5** 973 (1998).

[9] J.W. Connor, R.J. Hastie, and J.B. Taylor, Proc. Roy. Soc. London **A 365** (1979) 1.

[10] A. Pletzer, private communication.

[11] J.W. Connor, Plasma Phys. Control. Fusion **40** 531 (1998).